



# Overview of KSTAR

**S. W. Yoon<sup>a</sup>**, J. G. Kwak<sup>a</sup>, W. C. Kim<sup>a</sup>, W. H. Ko<sup>a</sup>, M. J. Choi<sup>a</sup>, H. Hahn<sup>a</sup>, J. Lee<sup>a</sup>, B. H. Park<sup>a</sup>, J. Chung<sup>a</sup>, W. Lee<sup>a</sup>, G. Y. Park<sup>a</sup>, H. H. Lee<sup>a</sup>, J. Kang<sup>a</sup>, S. -H. Hahn<sup>a</sup>, Y. In<sup>b</sup>, H. Park<sup>b</sup>, Y. S. Na<sup>c</sup>, J. M. Park<sup>d</sup>, J. Park<sup>e</sup>, Y. S. Park<sup>f</sup>, and the KSTAR Team<sup>a</sup>

<sup>a</sup> Korea Institute of Fusion Energy, Republic of Korea

<sup>b</sup> Ulsan National Institute of Science and Technology, Republic of Korea

<sup>c</sup> Seoul National University, Seoul, Republic of Korea

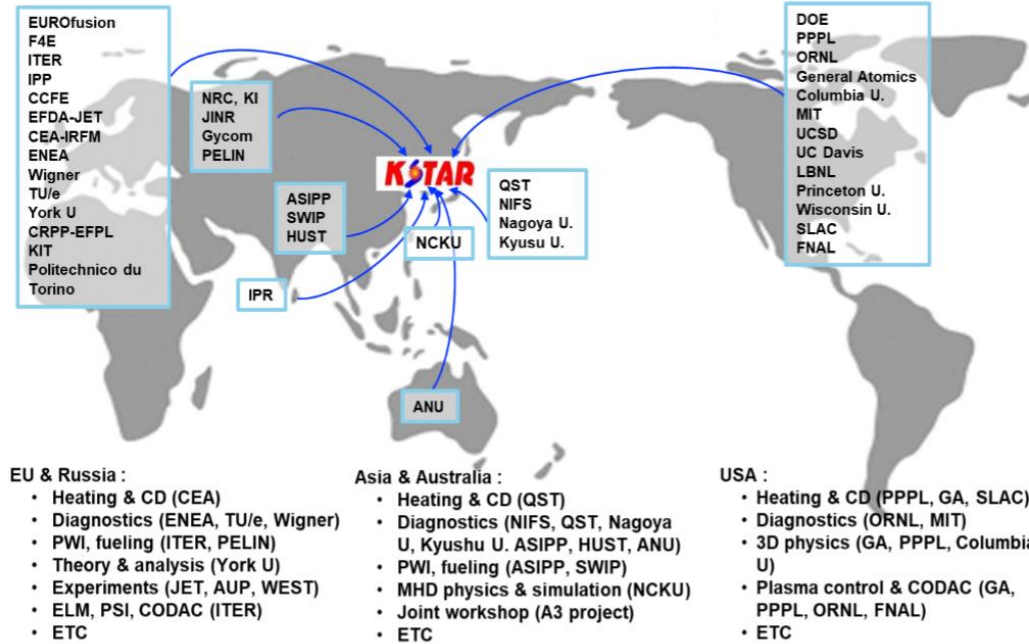
<sup>d</sup> Oak Ridge National Laboratory, USA

<sup>e</sup> Princeton Plasma Physics Laboratory, USA

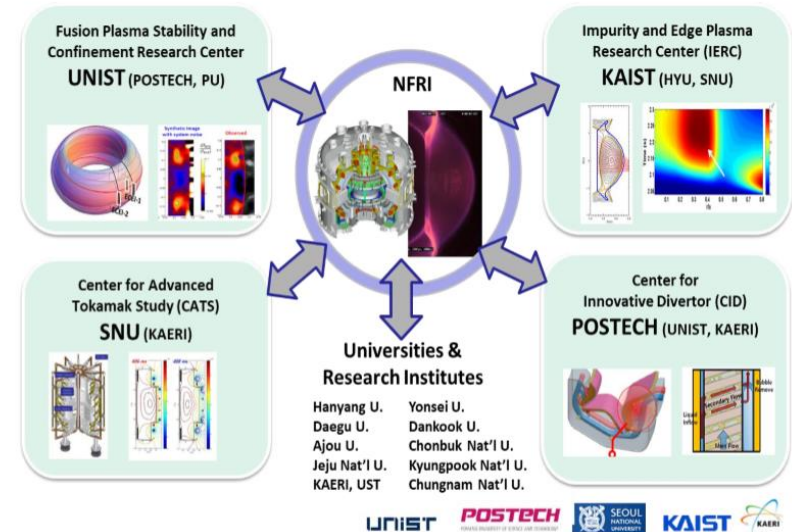
<sup>f</sup> Columbia University, USA

# Strong contributions from domestic and international collaborators

## International Collaborators



## Domestic Collaborators



## Acknowledgements

This research was supported by R&D Program of "KSTAR Experimental Collaboration and Fusion Plasma Research (EN2101-12)" through the Korea Institute of Fusion Energy (KFE) funded by the Government funds, and it was done also in collaboration with the ITER DMS Task Force and funded by the ITER Organization under contract IO/CT/43-1918.

- **Scenario development toward high beta steady-state operation**

Improved scenario control and extended operation windows at KSTAR

Further development for advanced scenario (*High  $q_{min}$ , Hybrid, high-Ti*)

- **3D field physics**

Optimal configuration of Resonant magnetic perturbation (RMP) ELM suppression

Validation of the plasma response and adaptive ELM control

- **Fundamental turbulence and transport**

Interaction of MHD & turbulence in transport

Turbulence spreading around magnetic island and avalanche-like transport

Effect of 3D field on transport and MHD

- **Disruption mitigation**

Diagnostics for the Shattered Pellet Injection

Experiments on multiple SPIs

# KSTAR is to address key physics and technical issues for ITER and DEMO

KSTAR superconducting fusion device

High frequency heating device (RF & microwave)

Neutral particle beam heating device (NBI-1 heating)

Plasma diagnostics device (Diagnostics)

C to W lower divertor upgrade in '2022

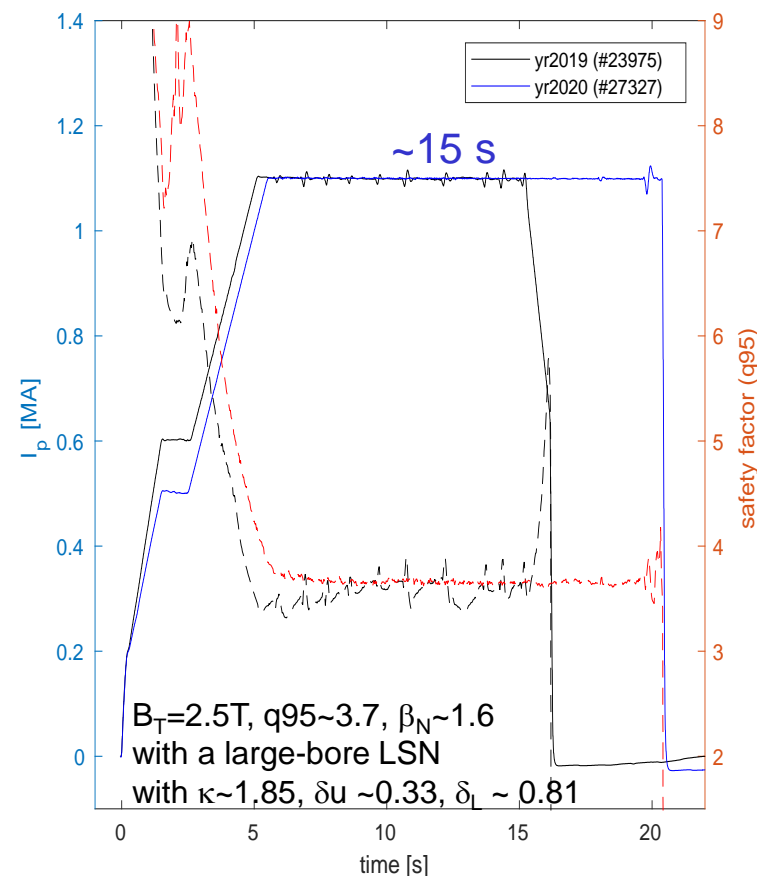
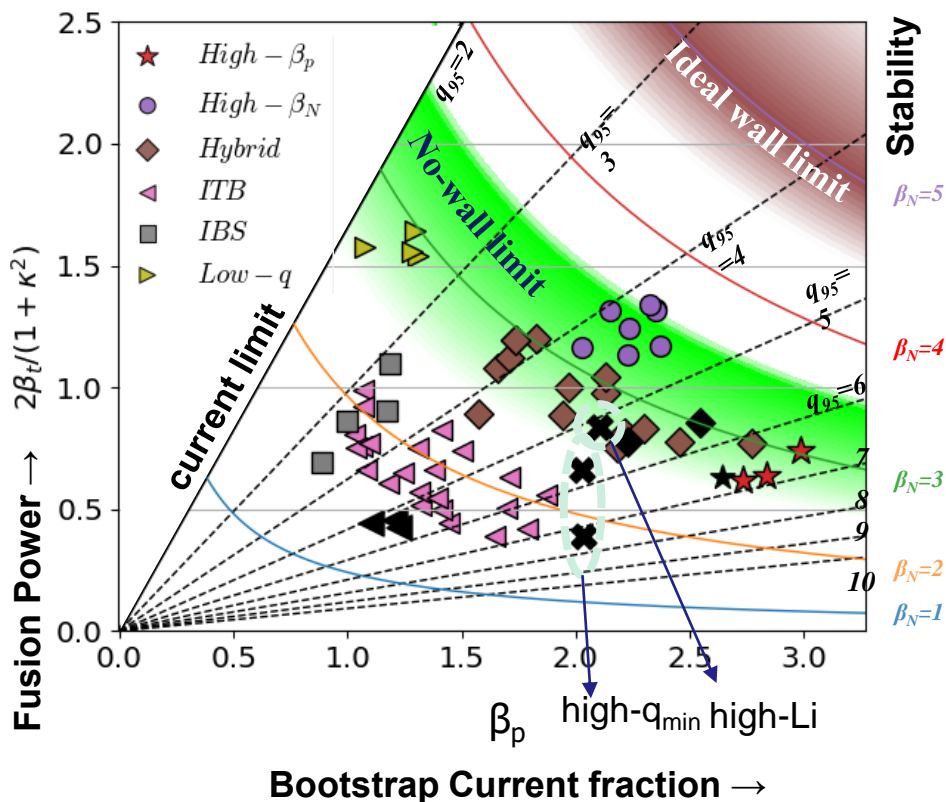
Expansion of heating device underway (NBI-2 upgrading)

Inside of vacuum vessel and plasma

Parameters	KSTAR (achieved)	ITER (Baseline)	K-DEMO (Option II)
Major radius, $R_0$ [m]	1.8 (←)	6.2	6.8
Minor radius, $a$ [m]	0.5 (←)	2.0	2.1
Elongation, $\kappa$	2.0 (2.16)	1.7	1.8
Triangularity, $\delta$	0.8 (←)	0.33	0.63
Plasma shape	DN, SN	SN	DN (SN)
Plasma current, $I_p$ [MA]	2.0 (1.0)	15	> 12
Toroidal field, $B_0$ [T]	3.5 (←)	5.3	7.4
H-mode duration [sec]	300 (70)	400	SS
$\beta_N$	5.0 (4.3)	~ 2.0	~ 4.2
Bootstrap current, $f_{bs}$	(~0.5)		~ 0.6
Superconductor	Nb <sub>3</sub> Sn, NbTi	Nb <sub>3</sub> Sn, NbTi	Nb <sub>3</sub> Sn, NbTi
Heating /CD [MW]	~ 28 (10)	~ 73	120
PFC	C, W	W	W
Fusion power, $P_{th}$ [GW]		~0.5	~ 3.0

# Overall performances in various operating scenarios

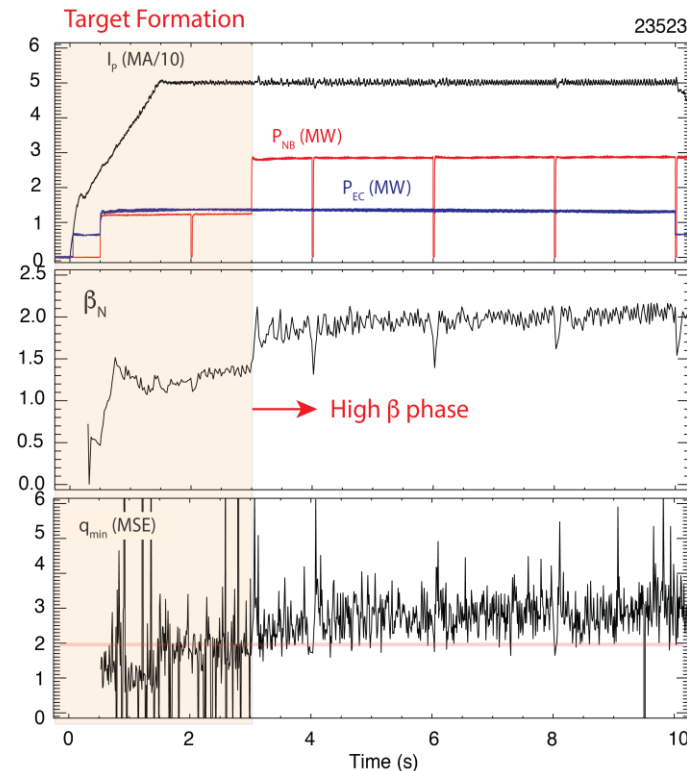
## High Ip plasma operation



Extension of operation regime continues with new controls (symmetry control, ECCD)

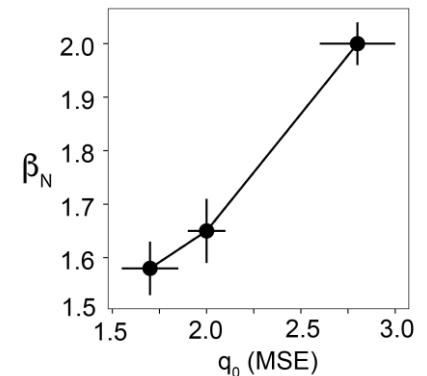
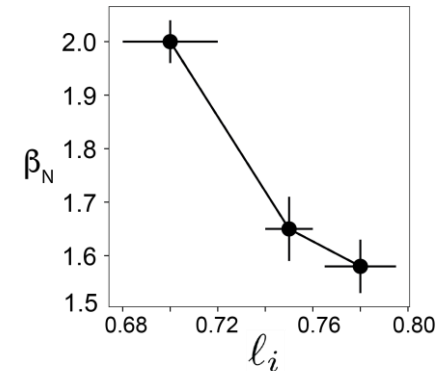
# Improved Access to High $q_{\min}$ ( $>2$ ) for High $\beta_N$ , Steady-State Scenario

- Access to high  $q_{\min}$ 
  - Early shaping
  - Early Heating & H-mode transition
- Slow  $\beta_N$  ramp during target formation
  - Minimize injection power and avoid MHD
  - Maintain high  $q_{\min}$
- Strong dependency of confinement on  $q_{\min}$ 
  - Improved confinement for broader current profile



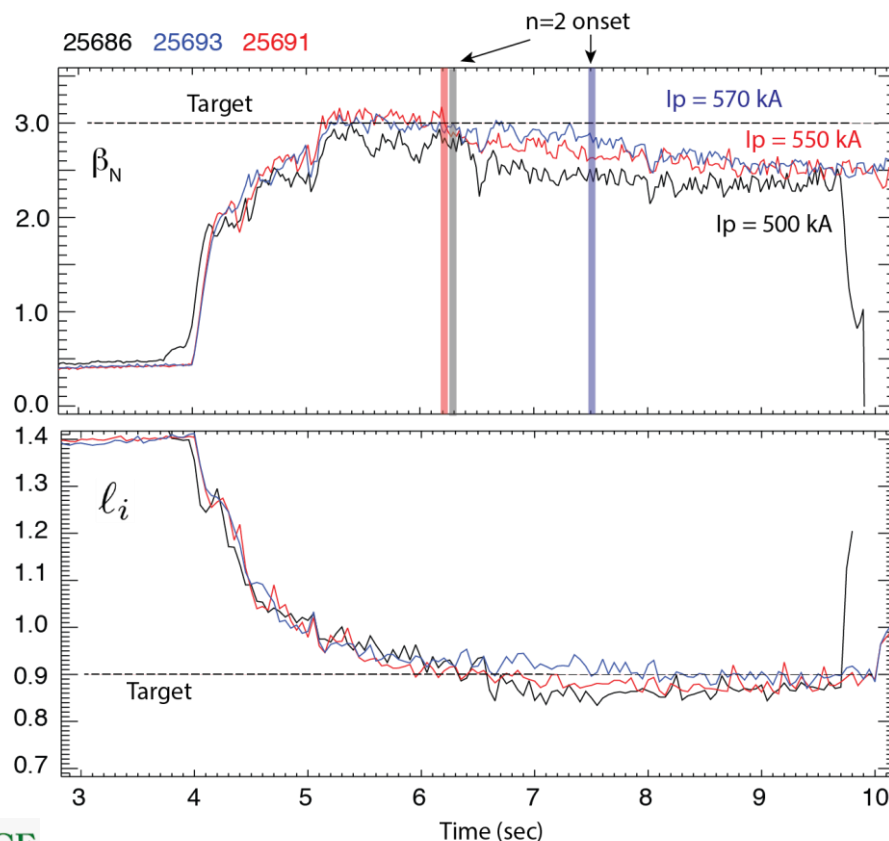
OAK RIDGE  
National Laboratory

J. M. Park, ORNL



# High Ii Scenario Achieves $\beta_N \approx 3$ , $V_{\text{Loop}} < 0$ at $q_{95} = 5$ but Transiently

- High performance, low  $q_{\text{min}} \approx 1$  scenario
  - Ohmic target formation and rapid  $\beta_N$  ramp at the highest Ii
  - Efficient on-axis CD (central ECCD + NB)
  - Maintain stability at high  $\beta_N$  w/o wall stabilization
- Robust shape control during rapid  $\beta_N$  ramp achieved
  - Feed-forward shape control of X-point target
  - Eliminate long ELM period between H-mode transition and first ELM: Preheating + gas puff
- $\beta_N > 3$  sustained until  $n = 2$  MHD onset
  - Confinement and mode onset time sensitive to  $I_p$  (or  $q_{95}$ )

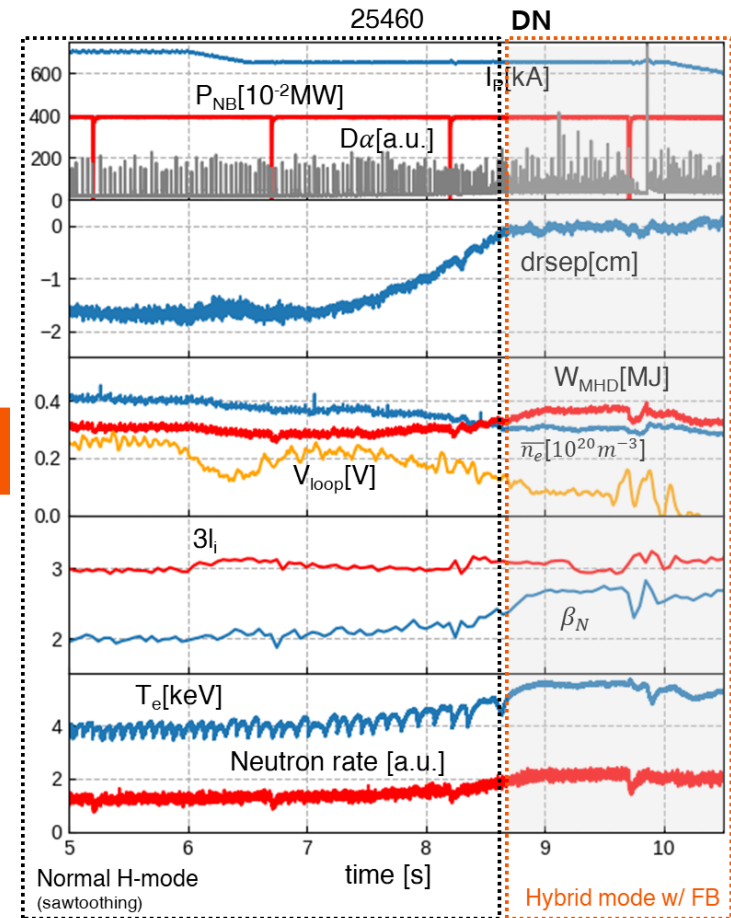
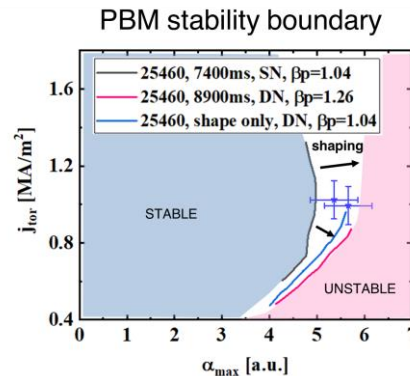
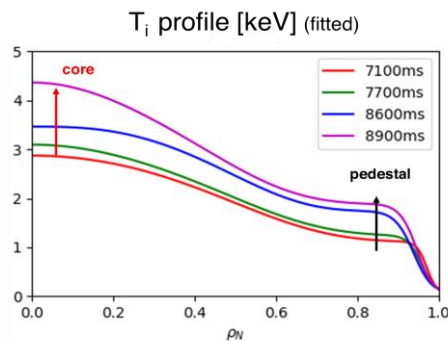
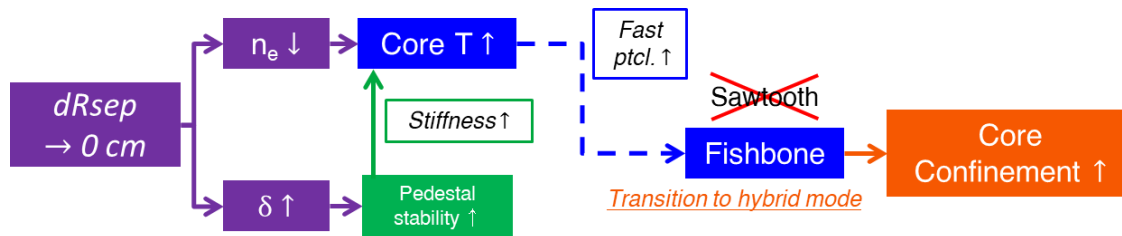


OAK RIDGE  
National Laboratory

J. M. Park, ORNL

# Transition to Hybrid mode by magnetic balance control

- In 2019-2020 experiments, transition from H- to hybrid mode was observed via dRsep control (-1.65cm → 0cm).
- #25460
  - $\beta_n = 2.0 \rightarrow 2.7$ ,  $V_{\text{loop}} = 0.2 \rightarrow 0.08$  V
  - **dRsep from -1.65 cm → 0** (DN in 8.7-10 s)
- Hypothesis for the mechanism of transition



# Long pulse sustainment(~30s) of Hybrid scenario

## ■ #25530

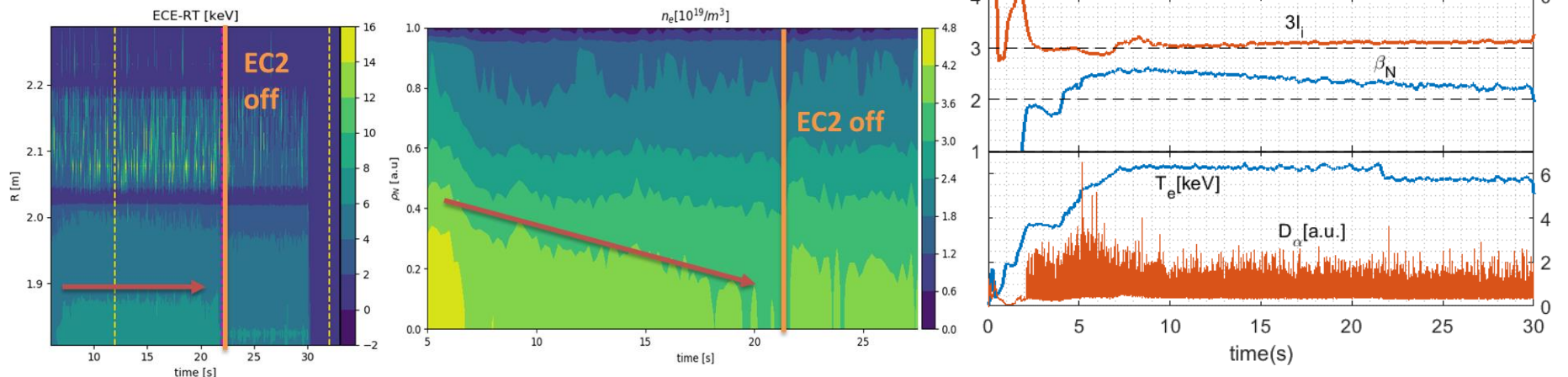
- Flattop sustained for **~30 s**
- $I_P = 0.6$  MA,  $P_{\text{total}} = 5.04$  MW
- $V_{\text{loop}} = 0.06\text{--}0.07$  V,  $I_i \sim 1.02$
- $T_e$  constant,  $n_e$  and  $T_i \searrow$ ,  $I_i \nearrow$



SEOUL  
NATIONAL  
UNIVERSITY

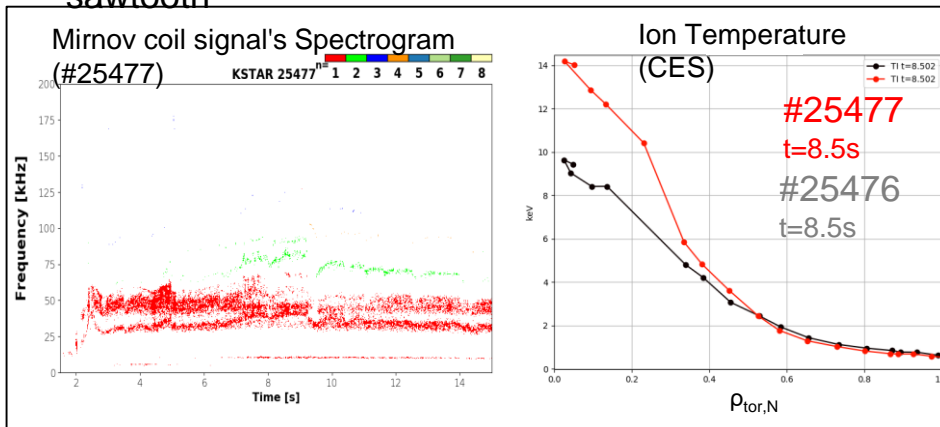
Y. S. NA, SNU

- The performance was gradually degraded with  $\beta_N = 2.6 \rightarrow 2.25$ , mainly due to density and ion temperature drop.

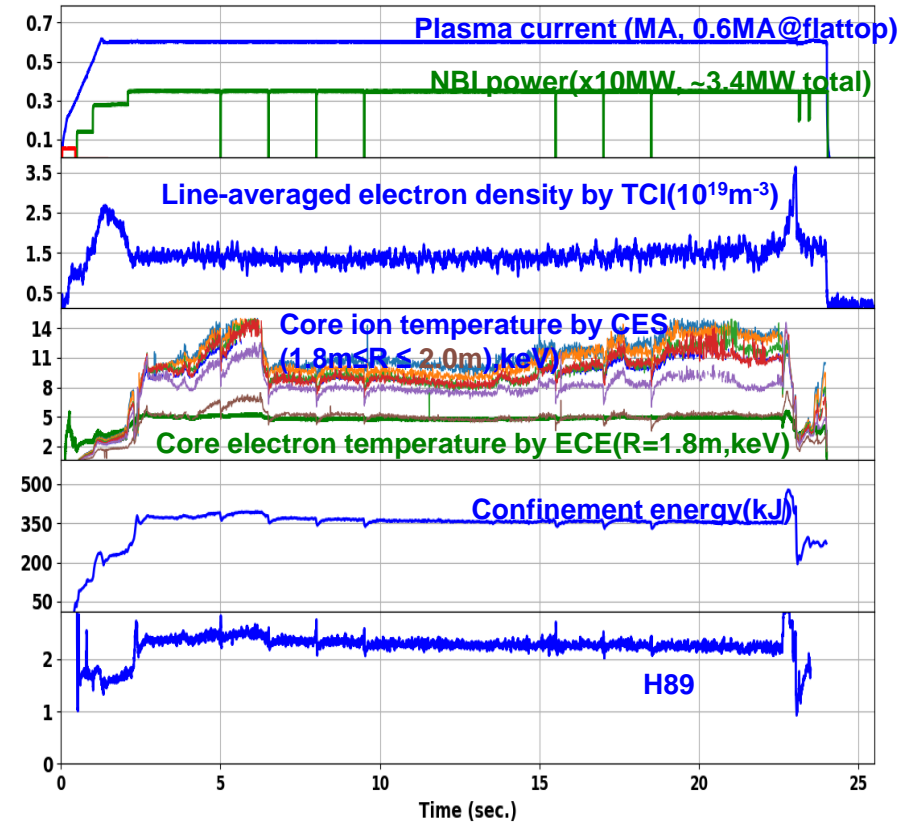


# Recent high Ti discharge in diverted L-mode edge

- Recently, KSTAR achieved stable diverted high  $T_i$  discharge (#25477) with L mode edge for ~ 20 s
  - $I_p = 0.6$  MA
  - $B_t = 1.8$  T
  - $q_{95} \sim 4.3$
  - $\beta_N \sim 2.2$
  - $H_{89L} \sim 2.3$
  - $T_{i0} > 10$  keV
- Almost fully non-inductive current drive with Loop voltage  $\sim 0.01$  V
- There are  $n=1$  energetic particle modes without sawtooth

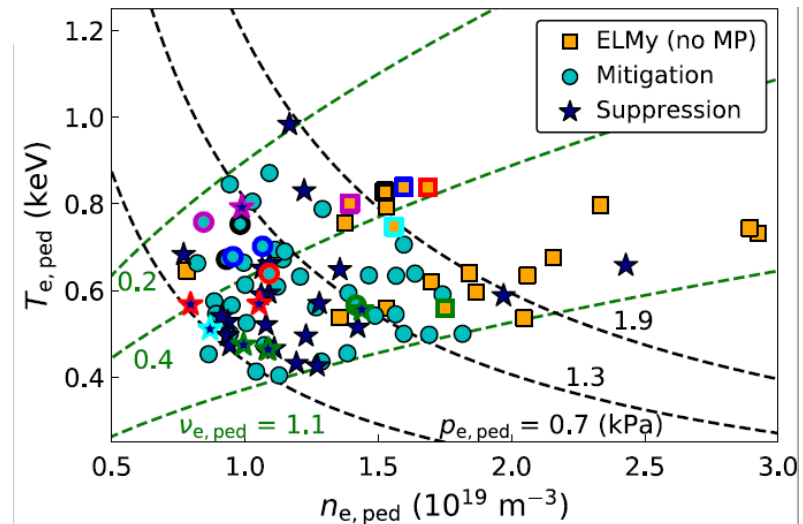
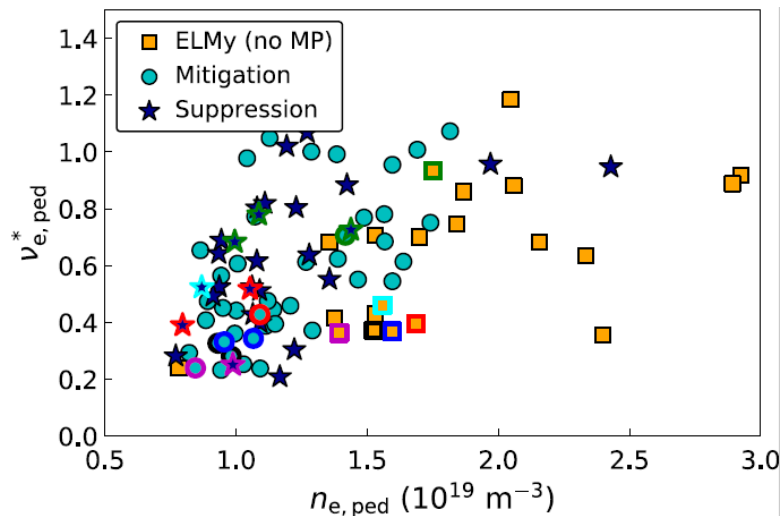


KSTAR #25860 (2020/10/16),  $B_t=1.8$ T



# RMP-driven, ELM suppressions in KSTAR show a rather scattered dependence of pedestal density and collisionality

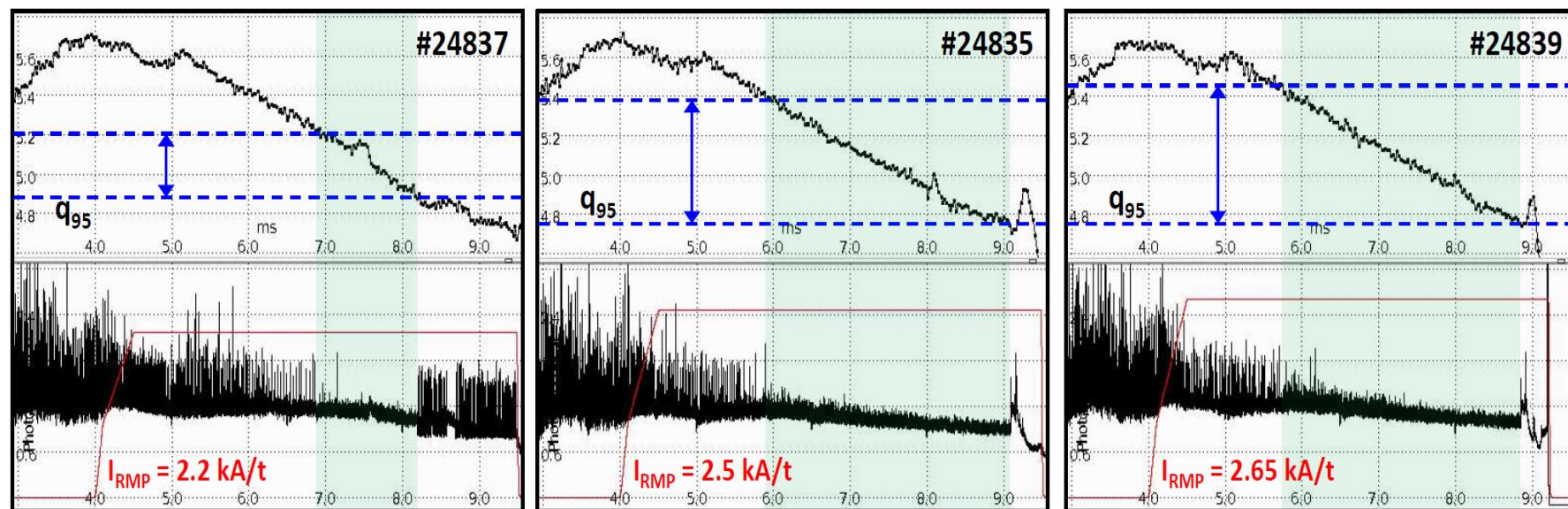
Empirically, low  $n_e$  and  $\nu^*$  plasmas are preferred for RMP-driven, ELM-crash-suppression



[M.W. Kim *et al*, to appear in Phys. Plasmas (2020)]

Nonetheless, no tendency is observed for RMP-driven, ELM-crash-suppression, according to the latest database in recent years (NOTE high  $n_e$  and  $\nu^*$  ELM suppression in KSTAR )

# As RMP amplitude increases, the $q_{95}$ window of $n=1$ RMP-driven, ELM suppression is expanded, consistent with theory



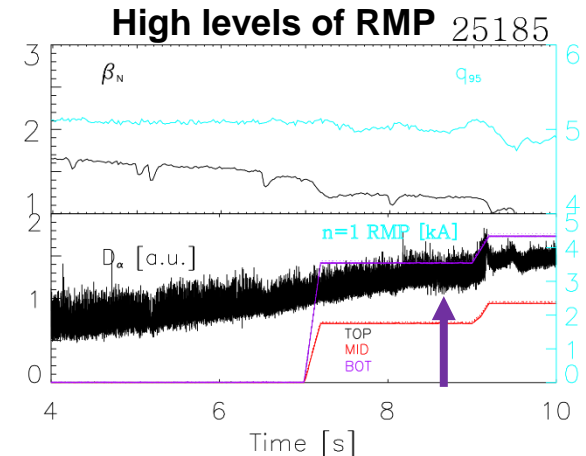
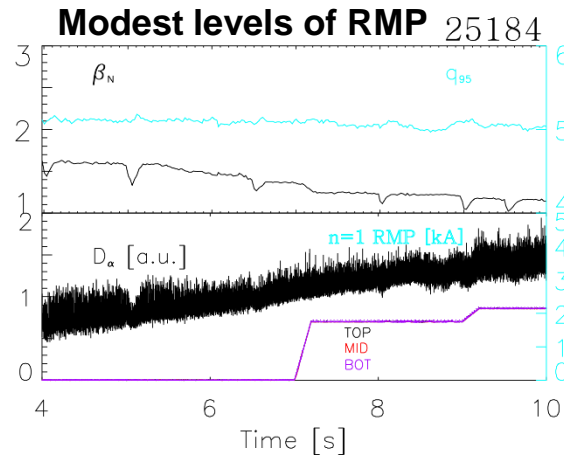
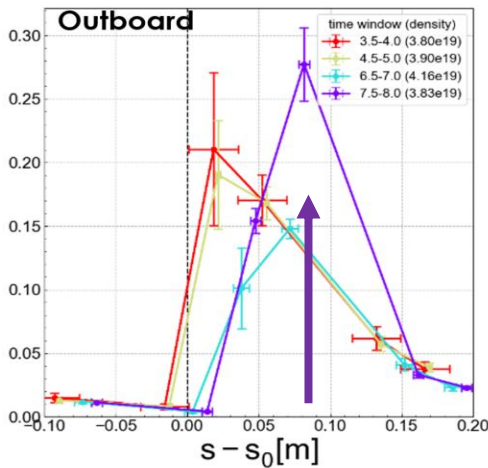
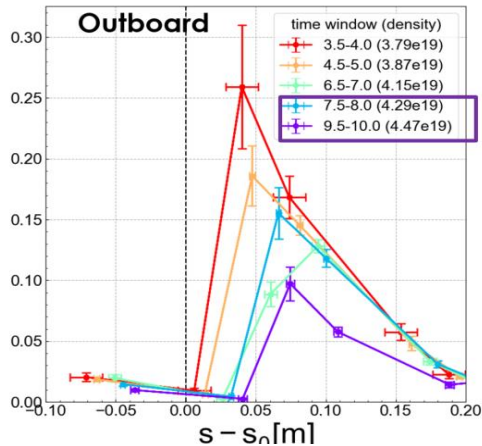
Once a large amplitude of RMP is utilized (without mode-locking), a wider range of  $q_{95}$  has been seen with RMP-driven, ELM-crash-suppression

[Y.M. Jeon, to be published (2020)]

-Predicted by TM1 [Q. Hu (PPPL)]



# High density plasma was successfully detached without impurity seeding, and has been sustained at modest level of RMP



[Y. In, H.H. Lee, J.H. Hwang *et al*, to be published (2020)]

However, at high level of RMP, the plasma gets re-attached, along with noticeable density pump-out

As expected [Frerichs *et al*, PRL (2020)], substantial reduction of the divertor heat fluxes have been measured in detached plasmas, even resulting in very low level of signal-to-noise ratio on IR camera



Y. In, UNIST

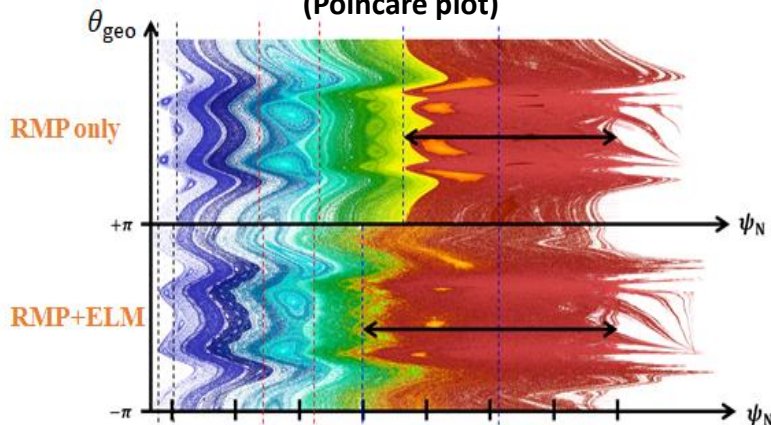


# Nonlinear RMP response contributes to the pedestal degradation and increased heat flux during RMP ELM control

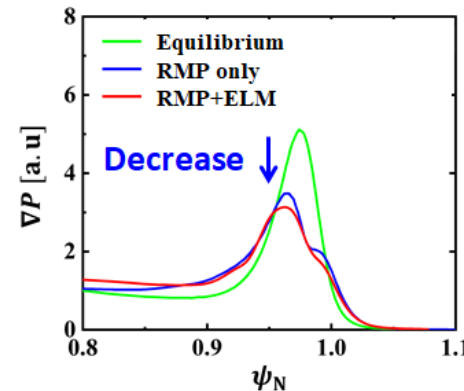
- Nonlinear 3D MHD modeling on KSTAR shows that RMP drives kink-tearing response, influencing the pedestal transport and divertor heat flux.
  - Degraded pedestal leads to increased background heat flux
- Plasma response can be changed by the MHD mode coupling with ELM.
  - Enhanced stochastic layer and pedestal transport by RMP-ELM coupling
  - Importance of mode coupling to fully describe the RMP-driven plasma response



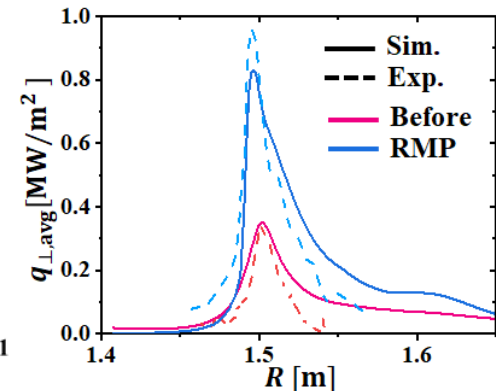
JOREK, KSTAR #18594 n=2  
(Poincare plot)



JOREK, KSTAR #18594 n=2  
(Pedestal degradation plot)



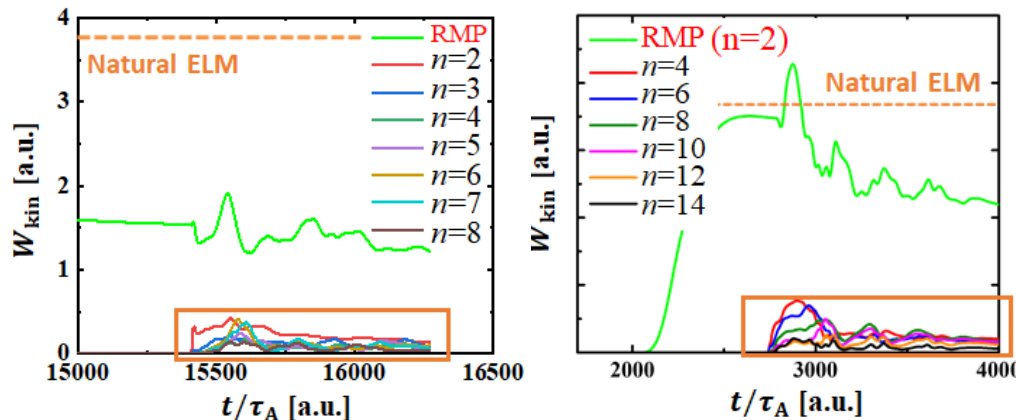
JOREK, Divertor heat flux  
(Lower LFS)



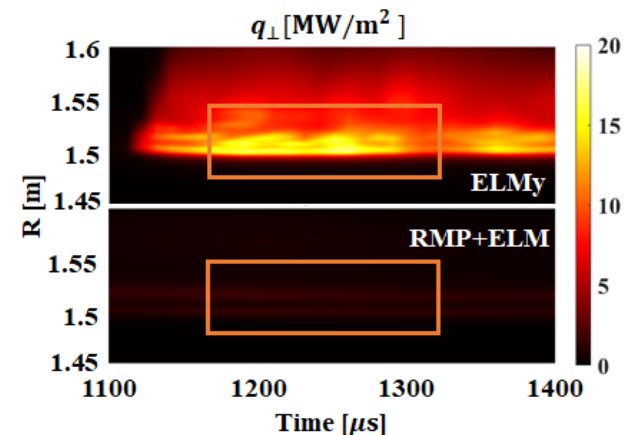
# RMP-driven ELM suppression is successfully reproduced with RMP+ELM+NTV integrated simulation

- Integrated MHD modeling shows that RMP ( $n=1,2$ ) can suppress ELM crashes
  - Full suppression of ELM burst
  - Significant reduction of bursty heat flux (But, 2 times larger background heat flux)
- NOTE that ELM crash suppression by RMP is the consequence of RMP response
  - Degraded pedestal gradient (Reduced instability source)
  - RMP-ELM mode coupling (Reduced bursty behavior ELM in nonlinear phase).

JOREK, ELM-crash suppression  
( $n=1$  #21072,  $n=2$  #18594)

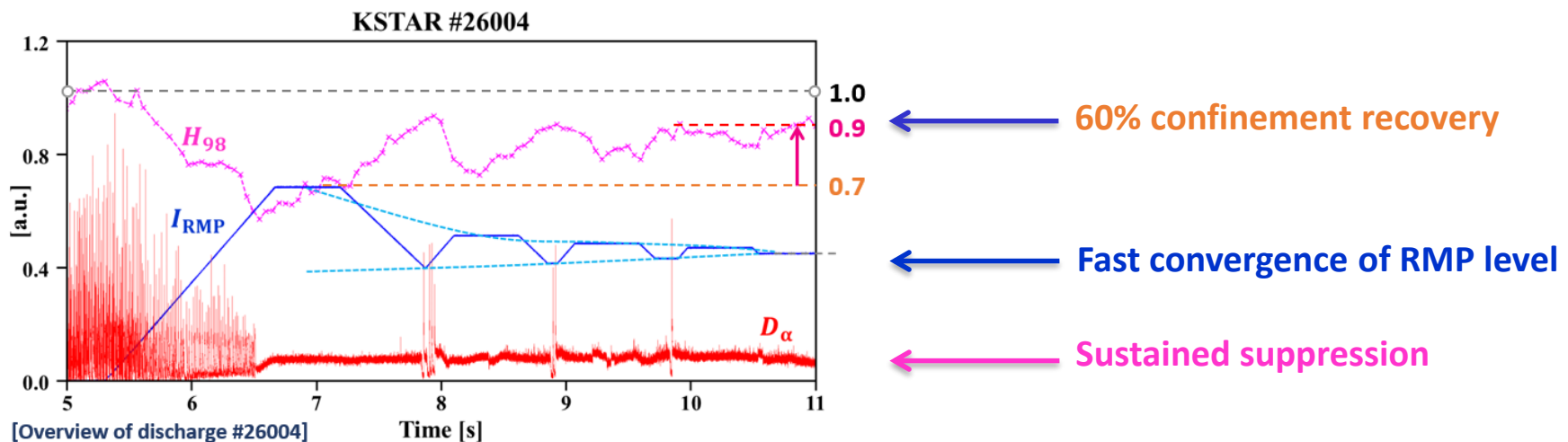


JOREK,  $n=1$  #21072  
(Disappeared ELM heat flux)



# Adaptive ELM control successfully optimizes the RMP level, maximizing the confinement recovery while maintaining ELM suppression

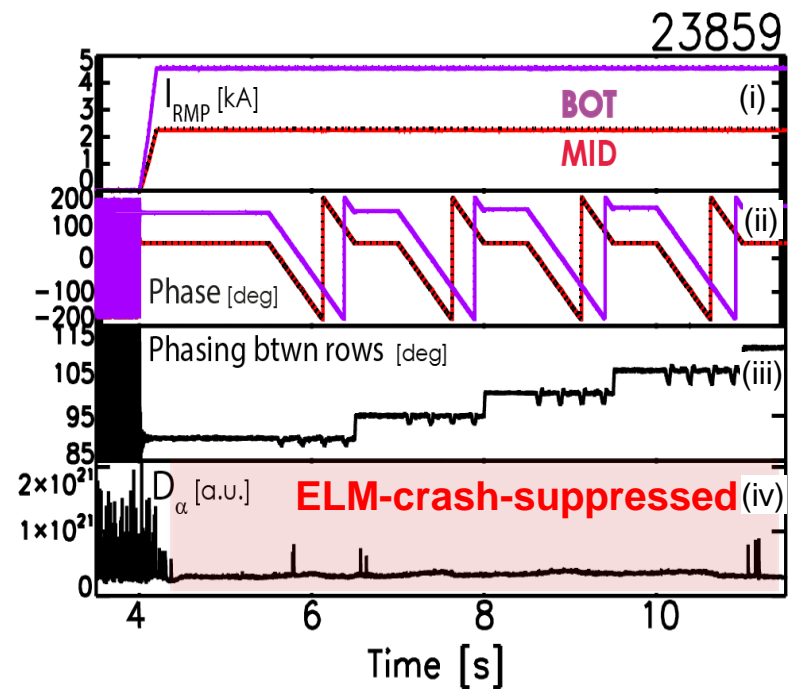
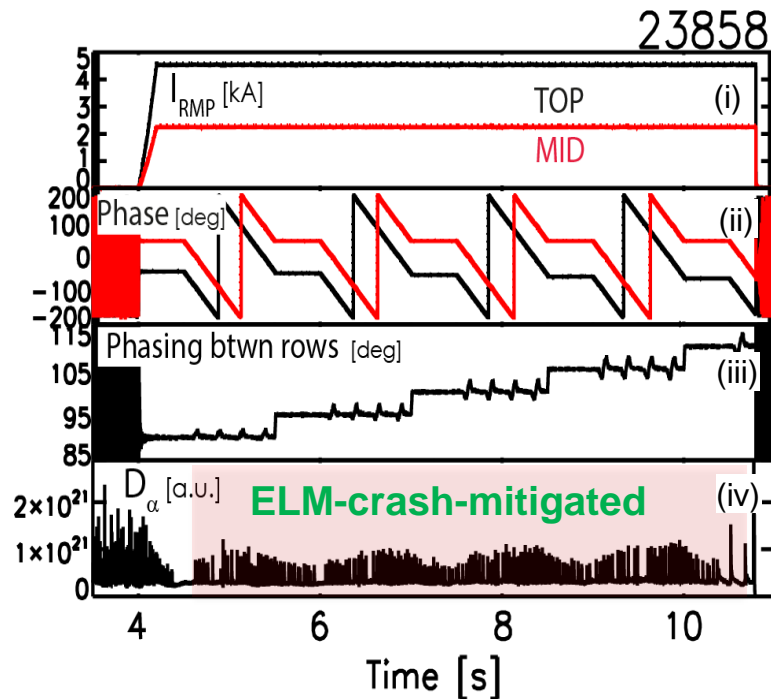
- ELM suppression with adaptive ELM control
  - ✓ Successful ELM suppression and confinement optimization by adaptive control.
  - ✓ **Recovered** confinement up to **60%** ( $H_{98} = 0.7 \rightarrow 0.9$ ).
  - ✓ Mainly due to stably/quickly **converged** RMP level.
  - ✓ Converged within 4 iterations, ~5 s.



Decreasing the RMP amplitude until the loss of ELM-crash-suppression (2.5 kA down to 1.7 kA), and then reversing the the RMP change for ELM-crash-suppression

[R. Shousha and S.K. Kim, to be published (2020)]

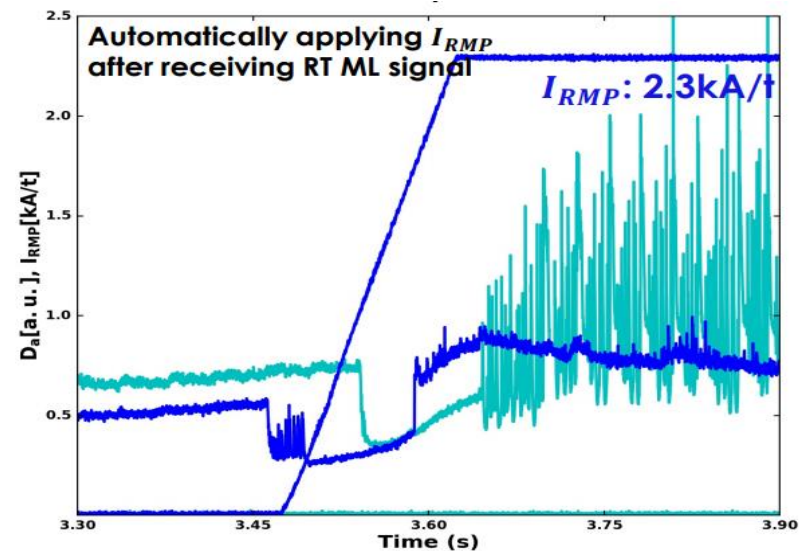
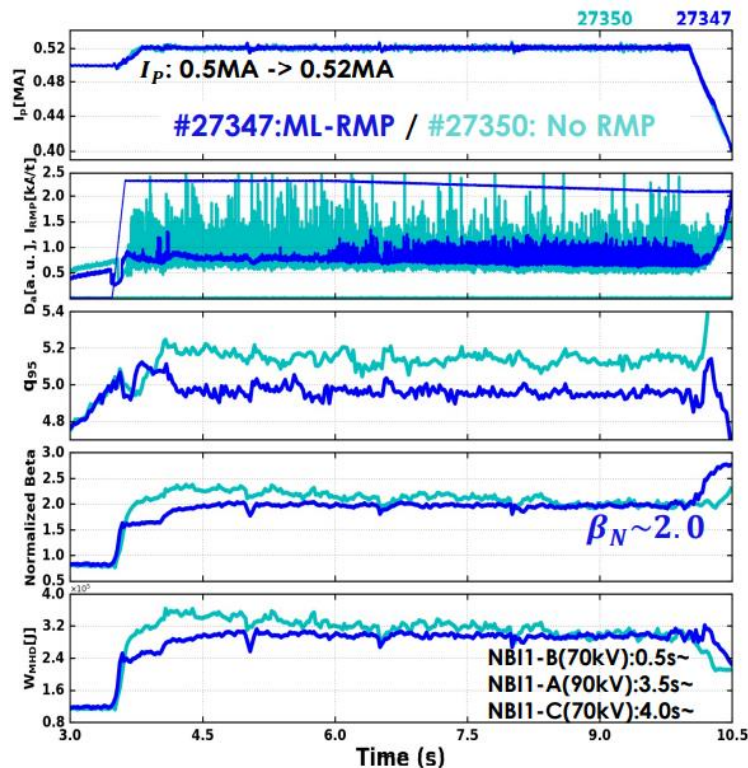
# Evidence of up/down asymmetric coupling difference for RMP ELM suppression, showing a meritorious use of Mid/Bot, instead of Top/Mid



- Potentially critical information for ITER RMP operation
- Much more reduced level of Bottom row was found to be sufficient, suggesting a weak coupling of top-row in 3-row IMCs

# Machine Learning (ML)-based RMP ELM control can successfully suppress first ELM right after L-H transition

- Real-time ML algorithm was shown to be working properly: classification + applying RMP
- First ELM** was successfully suppressed by applying RMP during ELM-free period right after the L-H transition
- ML-based method has positive effects on sustaining high-beta plasmas during the whole discharge period



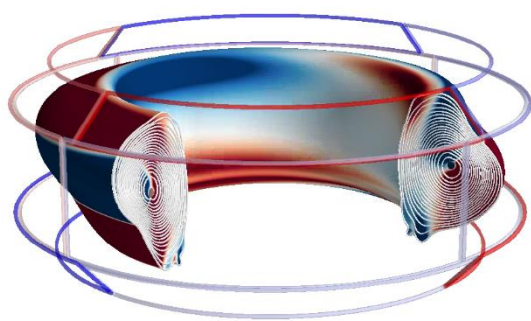
- First ELM suppression success
  - ✓ Adjust  $q_{95} \sim 5.0$
  - ✓ Increase  $I_{RMP}$ : 2.1  $\rightarrow$  2.3kA/t

# KSTAR is successfully testing a comprehensive error field correction scheme using a concept of QSMP

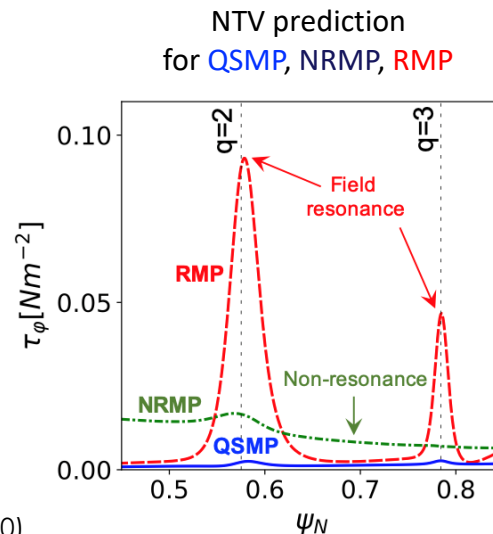
Quasi-symmetric magnetic perturbation (QSMP) in a tokamak: A 3D field that can induce minimum neoclassical 3D transport, compared to NRMP or RMP, as successfully tested in KSTAR and DIII-D

Implies: Error field can be modified towards QSMP in correction, to minimize both resonant or non-resonant effects – more comprehensive or alternative scheme in error field correction problems in tokamaks

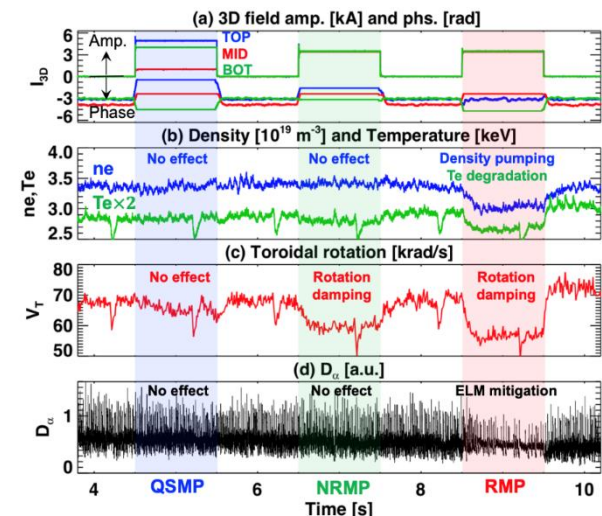
KSTAR QSMP configuration, with large dB but minimum impact on 3D transport



[1] J.-K. Park et al., PRL under review (2020)



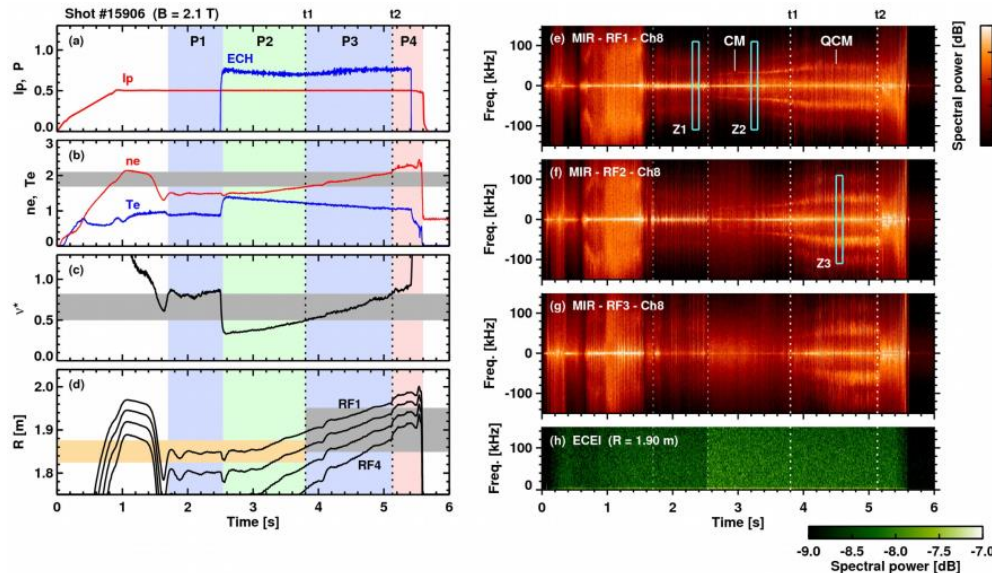
Experimental comparisons



# High-k scattering diagnostics provides key insight on relation between turbulence and MHD stability

## Transition of coherent mode to QCM

*W. Lee, accepted in NF & ibid (MF1-O11)*

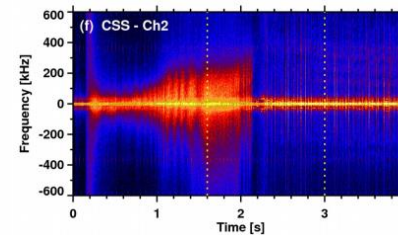


Collisional wavenumber broadening of coherent mode is a mechanism of the quasi-coherent spectrum

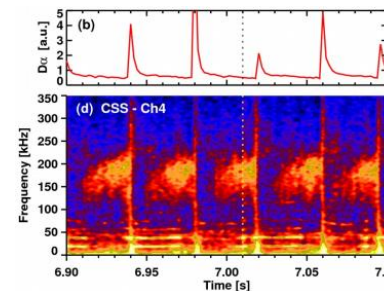
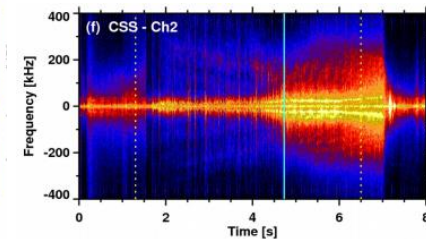
## High-k density fluctuations are now routinely measured by CSS diagnostics

*W. Lee, submitted to PPCF*

Turbulence suppression after LH transition



Turbulence increase with reduced ELM size



Gradual increase of turbulence before ELM crashes

# Nonlinear energy transfer provides key insight on relation between turbulence and MHD stability

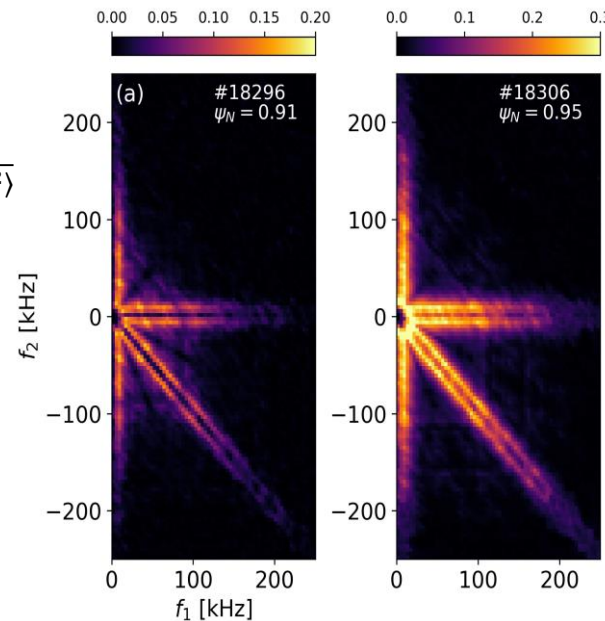
- Nonlinear three-wave coupling and energy transfer from ELM to broadband density turbulence during the ELM crash event

*J. Kim, NF 60, 124002 (2020)*

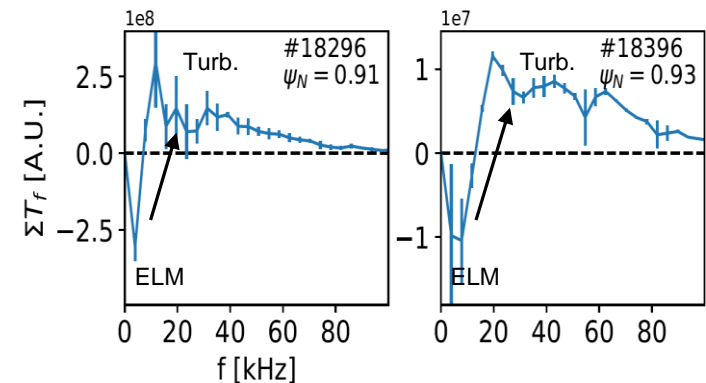
Squared-bicoherence

$$b^2(f_1, f_2) = \frac{|\langle F_n(f_1)F_n(f_2)F_n^*(f_1 + f_2) \rangle|^2}{\langle |F_n(f_1)F_n(f_2)|^2 \rangle \langle |F_n^*(f_1 + f_2)|^2 \rangle}$$

Strong bicoherence shows the nonlinear coupling between ELM and turbulence



Analysis of quadratic energy transfer rate [Ritz PFB 1989, de Wit JGRA 1999] revealed the direction of the energy transfer

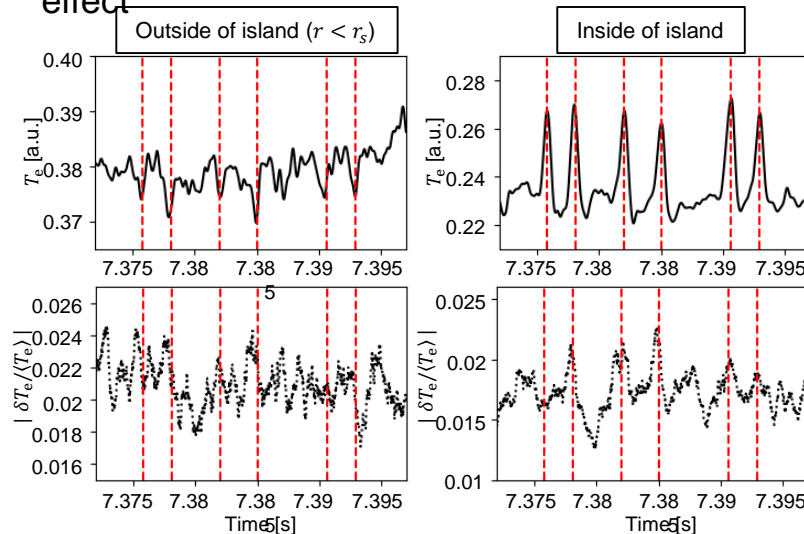


# Turbulence spreading around magnetic island : Rapid heat transport and reconnection inside island

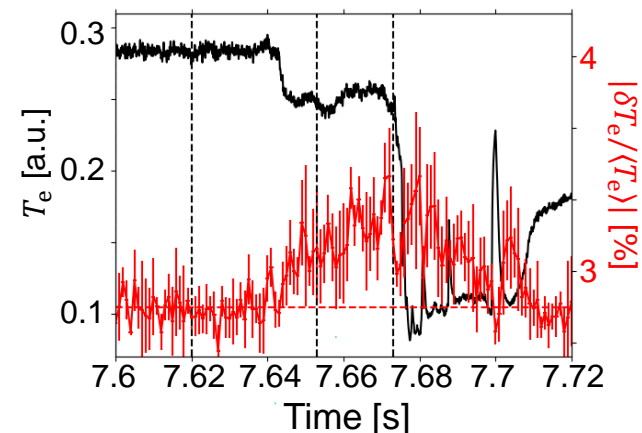
- Complex effects of the  $T_e$  turbulence on the magnetic island evolution

*M. Choi, submitted to Nature Comm.*

Spontaneous  $T_e$  peaking inside the island due to the turbulence spreading has a stabilizing effect



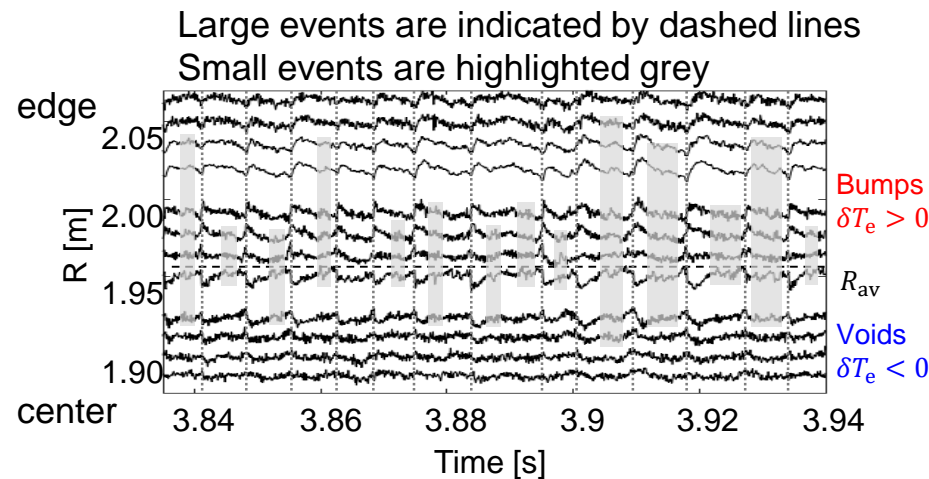
Turbulence enhancement at the reconnection site (X-point of the island) leads to the further reconnection and field stochastization, i.e. minor disruption.



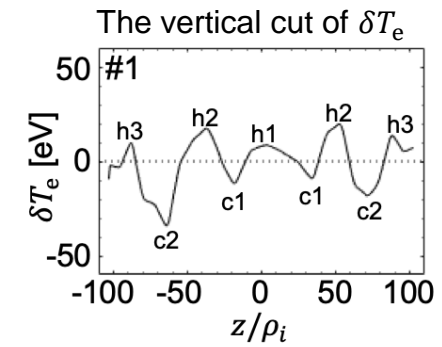
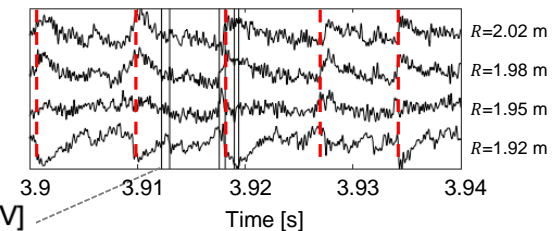
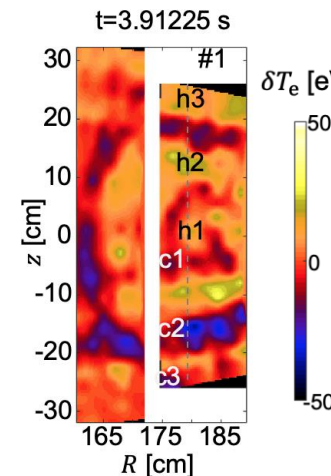
# ExB shear regulates Avalanche-like transport in L-mode (1)

- Avalanche-like heat transport events and their regulation by ExB shear flow layers in MHD quiescent KSTAR L-mode plasmas

M.J. Choi, NF 59, 086027 (2019) & *ibid* (F-I43)  
Large events



Te profile  
corrugation =  
shear flow layers

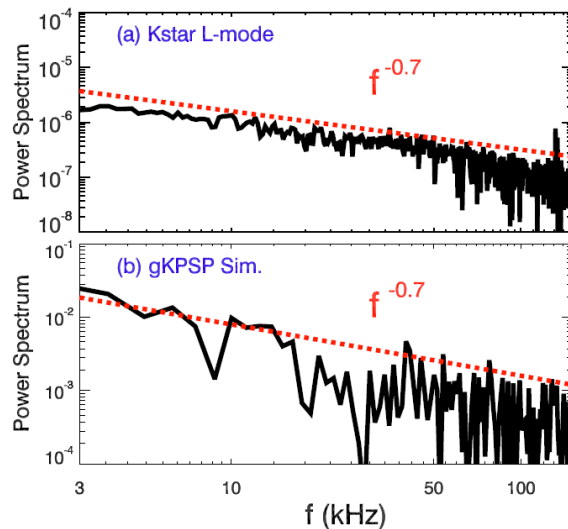


When shear layers exist, the size of the avalanche-like events is limited in the mesoscale ( $\sim 45\rho_i$ ).  
Large events occur after the shear layers are destroyed.

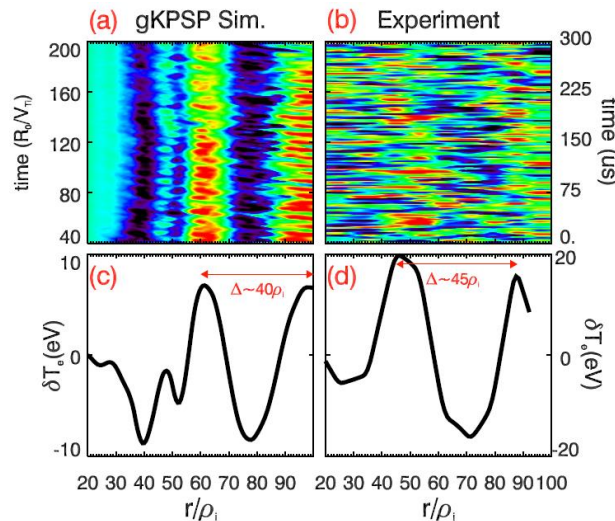
# ExB shear regulates Avalanche-like transport in L-mode (2)

- Gyrokinetic simulation of KSTAR L-mode plasmas reproduces electron heat avalanches and zonal ExB shear flow layers *L. Qi, submitted to NF*

Similar power-law spectra of  
avalanche  $T_e$  perturbations  
 $|\delta T_e(f)|^2: S(f) \sim f^{-0.7}$

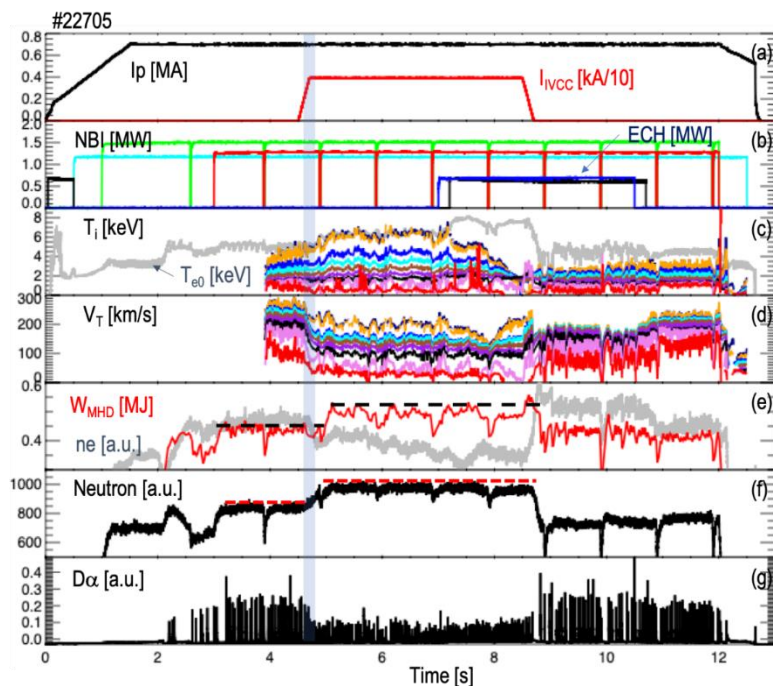


Quantitative agreement of the width  
of the profile corrugation



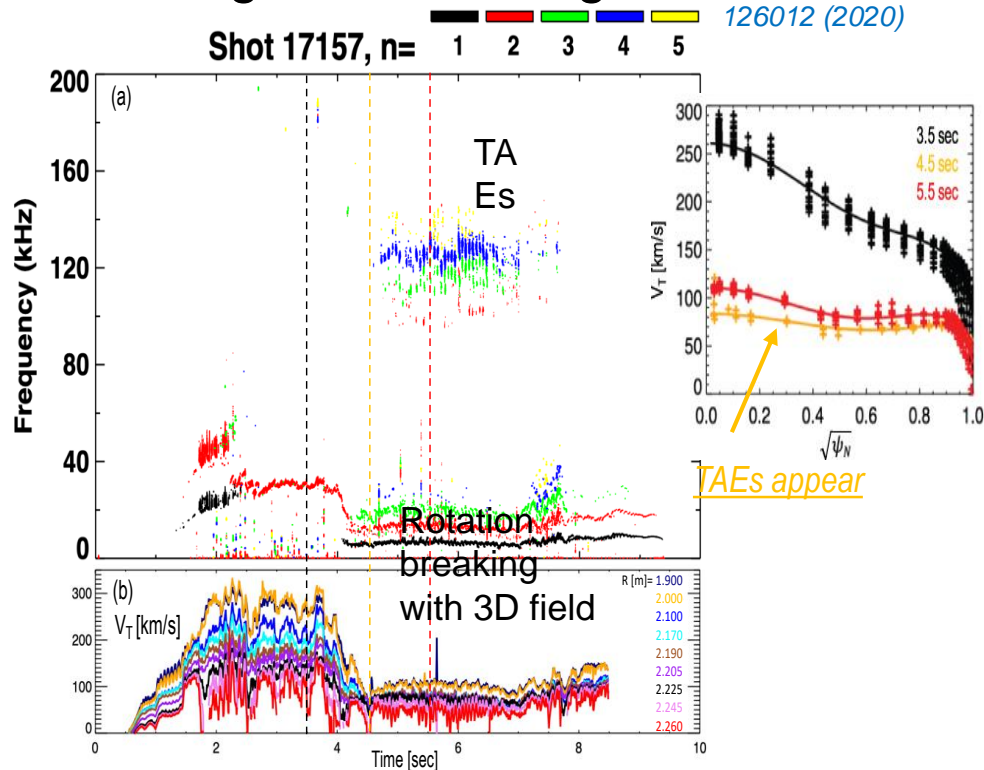
# 3D field effect on transport and Alfvén Eigenmodes

- 3D magnetic breaking improved energy confinement



- TAEs are destabilized by 3D magnetic breaking

K. Kim, NF 60, 126012 (2020)



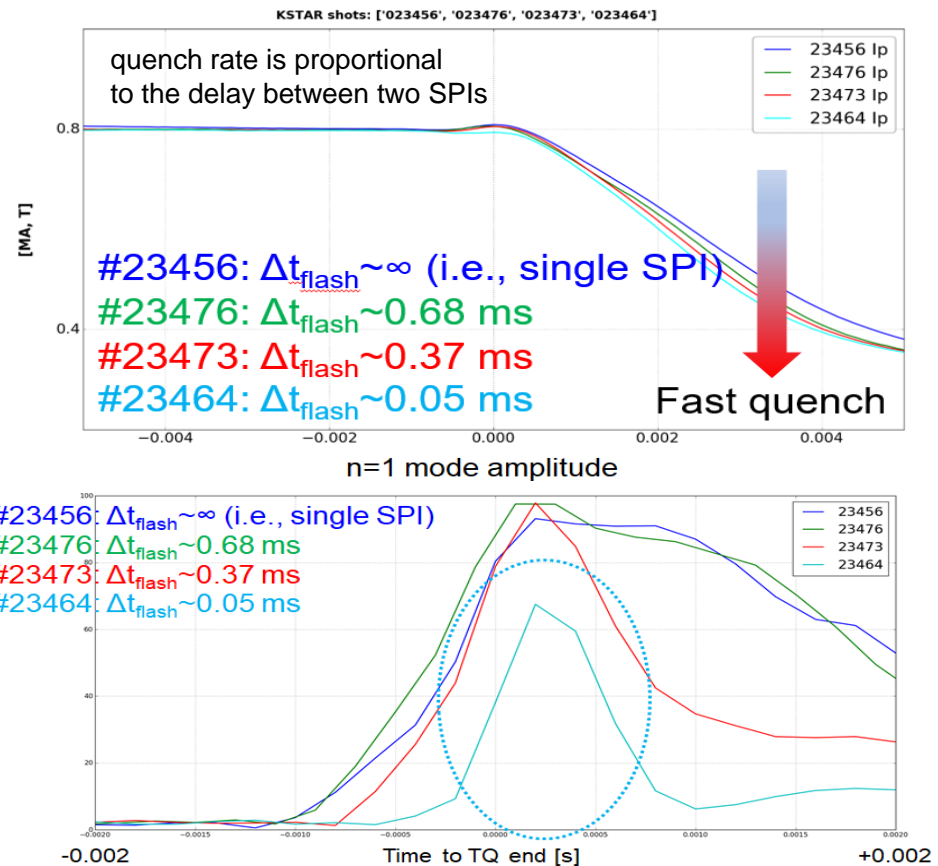
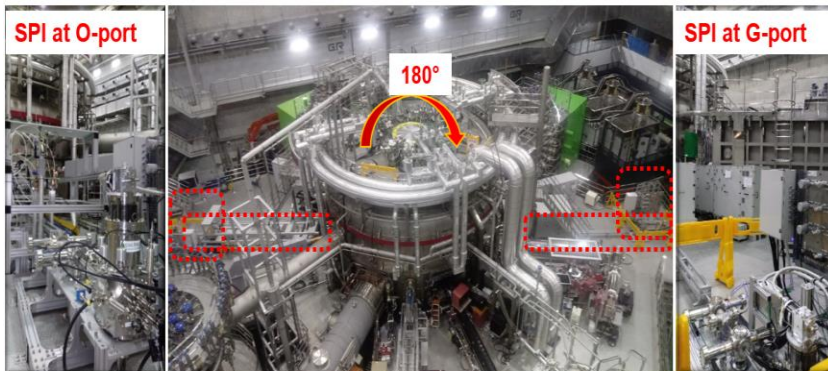
# KSTAR dual SPI experiments demonstrated the feasibility of simultaneous multiple injection planned in ITER

- Two identical SPIs were installed in toroidally opposite locations in KSTAR in collaboration among IO, ORNL, and NFRI

- Low Z ( $D_2$ ), high Z (Ne, Ar), and their mixture can be injected selectively.

- Three barrels in each SPI control the pellet size (i.e., amount of particles): 4.5 mm + 2x7.0 mm

- KSTAR volume:  $1.8 \times \pi \times (0.45)^2 \times 2 \times \pi \times 3.14 \times 1.8 \sim 12.9 \text{ m}^3$
- 4.5 mm:  $D\# = 2.18 \times 10^{21}$ ,  $Ne\# = 3.83 \times 10^{21}$ ,  $Ar\# = 5.37 \times 10^{21}$
- 7.0 mm:  $D\# = 8.77 \times 10^{21}$ ,  $Ne\# = 1.54 \times 10^{22}$ ,  $Ar\# = 2.16 \times 10^{22}$
- 8.5 mm:  $D\# = 1.60 \times 10^{22}$ ,  $Ne\# = 2.82 \times 10^{22}$ ,  $Ar\# = 3.96 \times 10^{22}$



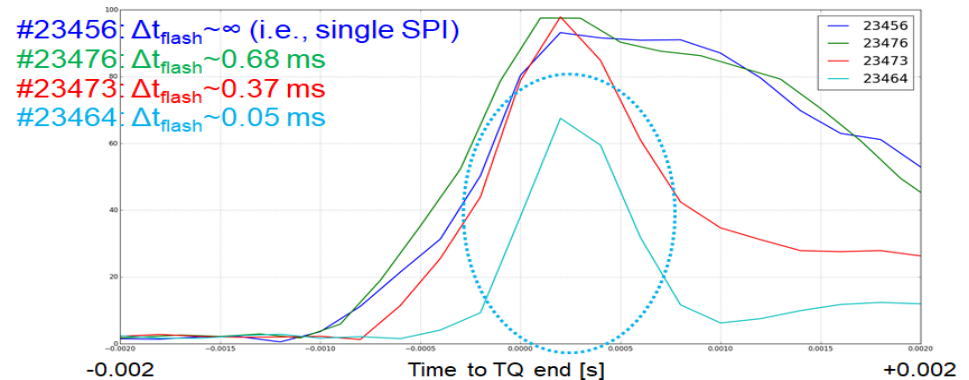
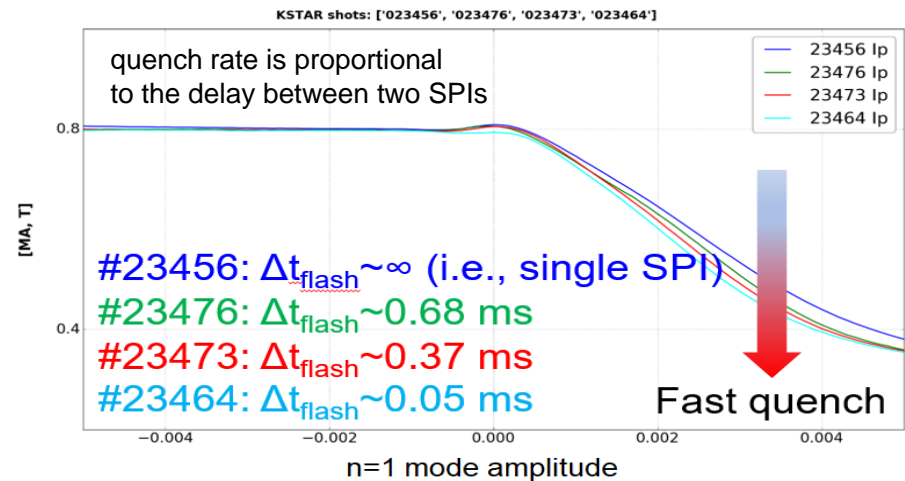
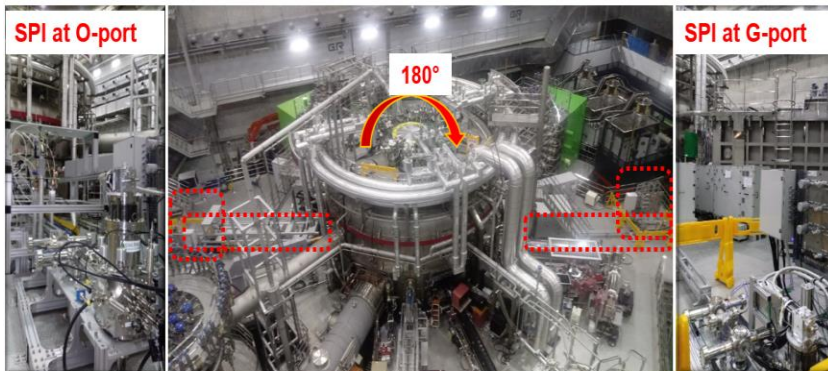
# KSTAR dual SPI experiments demonstrated the feasibility of simultaneous multiple injection planned in ITER

- Two identical SPIs were installed in toroidally opposite locations in KSTAR in collaboration among IO, ORNL, and NFRI

- Low Z ( $D_2$ ), high Z (Ne, Ar), and their mixture can be injected selectively.

- Three barrels in each SPI control the pellet size (i.e., amount of particles): 4.5 mm + 2x7.0 mm

- KSTAR volume:  $1.8 \times \pi \times (0.45)^2 \times 2 \times \pi \times 3.14 \times 1.8 \sim 12.9 \text{ m}^3$
- 4.5 mm:  $D\# = 2.18 \times 10^{21}$ ,  $Ne\# = 3.83 \times 10^{21}$ ,  $Ar\# = 5.37 \times 10^{21}$
- 7.0 mm:  $D\# = 8.77 \times 10^{21}$ ,  $Ne\# = 1.54 \times 10^{22}$ ,  $Ar\# = 2.16 \times 10^{22}$
- 8.5 mm:  $D\# = 1.60 \times 10^{22}$ ,  $Ne\# = 2.82 \times 10^{22}$ ,  $Ar\# = 3.96 \times 10^{22}$



# SUMMARY

- Enhanced performance in various operating regimes was obtained and machine parameters were expanded, including early diverting, sustainment of the centrally peaked high ion temperature mode, hybrid scenario, stationary high beta discharge and long-pulse H-modes
- Key issues for RMP ELM suppression has been further resolved focusing on the optimal poloidal spectrum, collisionality, and the real-time control capability for minimum performance degradation
- Cross-validation between the advanced diagnostics and the modeling provides new insight on the fundamental transport process including avalanche-like electron heat transport and QCM
- Providing unique demonstration on the performance of symmetric multiple Shattered Pellet Injections (SPIs) which is the main strategy of ITER for disruption mitigation